ESMO GOOD SCIENCE BETTER MEDICINE BEST PRACTICE

ESMO OPEN SCIENCE FOR OPTIMAL CANCER CARE

ORIGINAL ARTICLE

Genomic and transcriptomic analyses of residual invasive triple-negative breast cancer after neoadjuvant chemotherapy in the prospective MIRINAE trial (a randomized phase II trial of adjuvant atezolizumab plus capecitabine compared to capecitabine; KCSG-BR18-21)

S.-A. Im[1†], K. Park[2†], J. Koh[1], C. Park[1], K. H. Jung[3], J. Lee[4], H. K. Ahn[5‡], A. Lee[6], S. H. Sim[7], M. H. Kim[8], J. H. Kim[9], J. H. Kim[10], K. E. Lee[11], K. H. Park[12], J. Bae[5], M. H. Lee[13], S. Lim[14], H. J. Kim[15], D.-W. Lee[1], J. H. Jeong[3], K. S. Lee[7], J. Sohn[8], K. J. Suh[9], J.-Y. Kim[16], Y. J. Cha[17], J. Moon[18], C.-Y. Ock[18], S.-B. Kim[3], K. Shin[4], H. Chae[7,9], G. M. Kim[8], K.-H. Lee[1], W.-Y. Park[2], Y. H. Park[16*] & I. H. Park[19*], Korean Cancer Study Group (KCSG) Breast Cancer Committee

[1]Seoul National University Hospital, Cancer Research Institute, Seoul National University College of Medicine, Seoul; [2]Samsung Genome Institute, Samsung Medical Center, Seoul; [3]Department of Oncology, Asan Medical Center, University of Ulsan College of Medicine, Seoul; [4]Division of Medical Oncology, Department of Internal Medicine, Seoul St. Mary's Hospital, College of Medicine, The Catholic University of Korea, Seoul; [5]Division of Medical Oncology, Department of Internal Medicine, Gachon University Gil Medical Center, Incheon; [6]Department of Hospital Pathology, Seoul St. Mary's Hospital, College of Medicine, Catholic University, Seoul; [7]Center for Breast Cancer, National Cancer Center, Goyang; [8]Division of Medical Oncology and Department of Internal Medicine, Severance Hospital, Yonsei University College of Medicine, Seoul; [9]Department of Internal Medicine, Seoul National University Bundang Hospital, Seoul National University College of Medicine, Seongnam; [10]Division of Medical Oncology, Department of Internal Medicine, Gangnam Severance Hospital, Yonsei University College of Medicine, Seoul; [11]Department of Hematology and Oncology, Ewha Womans University Hospital, Seoul; [12]Division of Hemato-Oncology, Department of Internal Medicine, Korea University College of Medicine, Korea University Anam Hospital, Seoul; [13]Department of Internal Medicine, Inha University Hospital, Incheon; [14]Department of Hemato-Oncology, Wonju Severance Christian Hospital, Yonsei University Wonju College of Medicine, Wonju; [15]Division of Oncology and Hematology, Department of Internal Medicine, Soonchunhyang University Cheonan Hospital, Cheonan; [16]Division of Hematology-Oncology, Department of Medicine, Samsung Medical Center, Sungkyunkwan University School of Medicine, Seoul; [17]Department of Pathology, Gangnam Severance Hospital, Yonsei University College of Medicine, Seoul; [18]Lunit, Seoul; [19]Division of Oncology, Department of Internal Medicine, Korea University Guro Hospital, Seoul, Republic of Korea

Available online xxx

Background: Profiling residual disease after neoadjuvant chemotherapy (NAC) might identify molecular target and tumor microenvironmental features to guide adjuvant therapy. We explored the characteristics of residual triple-negative breast cancer (TNBC) in the prospective MIRINAE trial (KCSG-BR18-21), a phase II study evaluating adjuvant atezolizumab plus capecitabine versus capecitabine in TNBC without pathological complete response after NAC (NCT03756298) through multi-omics analyses.

Materials and methods: Residual TNBC samples were analyzed for tumor-infiltrating lymphocytes (TILs), programmed death-ligand 1 (PD-L1) immunohistochemistry (IHC), and Lunit SCOPE IO immune phenotype (IP). Mutations were assessed by FoundationOne®CDx, and RNAseq was conducted for molecular subtyping and gene expression analyses.

Results: Three hundred and five patients were analyzed, and ypTNM (post-neoadjuvant pathological tumor—node—metastasis) stages were stage I (28.0%), II (48.7%), and III (23.3%). High TILs were observed in 27.1% and PD-L1 IHC was positive in 39.5%. Pathogenic alterations in *TP53*, phosphatidylinositol 3-kinase (PI3K)/protein kinase B (AKT), and homologous recombination repair (HRR) pathways were observed in 86.3%, 27.1%, and 11.9%. Most patients were basal-like (51.1%) by PAM50, and mesenchymal (MES; 36.7%) or basal-like immune suppressed (BLIS; 30.3%) by TNBC molecular classification. TIL-high group was enriched with the basal-like immune-activated (BLIA) subtype (37.5%), with up-regulation of immune response-related gene sets. Nineteen patients (6.2%) recurred within 6 months of surgery (6.2%), mostly being basal-like (85.7%) or BLIS (64.3%), with low TILs and desert IP.

*Correspondence to: Prof. Yeon Hee Park, Division of Hematology-Oncology, Department of Medicine, Samsung Medical Center, Sungkyunkwan University School of Medicine, 81 Irwon-ro, Gangnam-gu, Seoul 06351, Republic of Korea. Tel: +82-2-3410-1780; Fax: +82-2-3410-1757
E-mail: yhparkhmo@skku.edu (Y. H. Park).
Prof. In Hae Park, Division of Hematology/Oncology, Department of Internal Medicine, Korea University Guro Hospital, Korea University College of Medicine, 148, Gurodong-ro, Guro-gu, Seoul 08308, Republic of Korea. Tel: +82-2-2626-3172
E-mail: parkih@korea.ac.kr (I. H. Park).

†Equally contributed as co-first authors.
‡Present address: Division of Hematology-Oncology, Department of Medicine, Samsung Medical Center, Sungkyunkwan University School of Medicine, Seoul 06351, Republic of Korea.

2059-7029/© 2025 The Author(s). Published by Elsevier Ltd on behalf of European Society for Medical Oncology. This is an open access article under the CC BY-NC-ND license (http://creativecommons.org/licenses/by-nc-nd/4.0/).

Up-regulations of *CCNE1*, *CD44*, and *BRD4* along with DNA replication-related gene sets were associated with early recurrence.
Conclusion: Residual TNBCs after standard NAC were predominantly basal-like or MES/BLIS subtypes with variable tumor microenvironment (TME). Early recurrence was associated with immune-cold TME, and further analyses on each treatment arm will provide deeper insights into the role of adjuvant immunotherapy.
Key words: triple-negative breast cancer, tumor-infiltrating lymphocyte, PD-L1, targeted sequencing, RNAseq

INTRODUCTION

Triple-negative breast cancer (TNBC) accounts for ∼15%-20% of all breast cancers and is characterized by the absence of estrogen receptor, progesterone receptor, and human epidermal growth factor receptor 2 (HER2) expression.[1] TNBC is known for its aggressive behavior, including a higher metastatic potential, early recurrence, and a lack of druggable targets. However, advancements in next-generation sequencing technologies have uncovered key characteristics of TNBC that may serve as potential targets for systemic treatment. Notably, the intratumoral heterogeneity of TNBC can be classified into distinct subtypes, some of which are associated with immune cell enrichment and are amenable to immunotherapy.[2,3] Additionally, *BRCA1*/2 mutations and homologous recombination deficiency (HRD) in TNBC contribute to unique tumor microenvironment (TME) modulation, and targeting HRD with agents such as poly (ADP-ribose) polymerase inhibitors may modulate TME to recruit active immune cells.[4] These insights have provoked ongoing investigations aimed at improving treatment strategies for TNBC patients.

For patients with stage II/III TNBC, neoadjuvant chemotherapy (NAC) is the preferred approach, offering both therapeutic benefits and prognostic information. Achieving pathological complete response (pCR) is associated with favorable long-term outcomes, whereas residual disease (RD) correlates with a high risk of recurrence and poor survival.[5] Consequently, the development of NAC regimens to increase pCR rates has been a key focus of TNBC treatment. Until recently, standard NAC regimens, combining anthracycline, taxane, and platinum agents, achieve pCR rates of ∼30%-50%.[6] In addition to this, the KEYNOTE-522 clinical trial demonstrated that adding pembrolizumab, an immune checkpoint inhibitor (ICI), to NAC significantly increased pCR rates to 64.8% and improved event-free survival and overall survival, leading to the integration of NAC plus ICIs as a standard treatment for early-stage TNBC.[7-9]

Despite these advancements, a significant proportion of patients fail to achieve pCR and require effective post-surgical treatment strategies. The CREATE-X trial established that adjuvant capecitabine significantly improved disease-free survival in patients without pCR after NAC.[10] However, the role of adjuvant immunotherapy in the post-NAC setting remains unclear, as most clinical trials investigating adjuvant ICIs, such as the ALEXANDRA/IMpassion030 trial, have focused on TNBC patients who did not receive NAC, making their results less directly applicable to the post-NAC RD setting.[11] This highlights the need for further investigation into the biology of residual TNBC to guide the development of optimal adjuvant strategies.

The MIRINAE trial (KCSG-BR18-21) is a randomized phase II prospective multicenter trial evaluating the efficacy and safety of adjuvant atezolizumab plus capecitabine versus capecitabine in TNBC patients who do not achieve pCR after NAC without immunotherapy (NCT03756298). While the clinical outcomes of the MIRINAE trial will be reported upon reaching the pre-defined statistical analysis point, understanding the molecular characteristics of residual TNBC remains a critical unmet need. Therefore, in parallel with the clinical trial, we conducted a comprehensive translational biomarker study to characterize residual TNBC using multi-omics analyses, including TME profiling and genomic characterization. Through this study, we aim to identify predictive and prognostic biomarkers associated with treatment efficacy, providing insights that may inform future therapeutic strategies for high-risk TNBC patients.

MATERIALS AND METHODS

Study scheme

Patients with TNBC who received anthracycline and taxane-based NAC followed by curative surgical resection were screened, and those found to have residual invasive carcinoma measuring ≥1.0 cm, with or without regional lymph node metastases, were enrolled.

Adjuvant atezolizumab (1200 mg every 3 weeks) for 1 year in addition to capecitabine (1000 mg/m^2 twice a day for 14 days, every 3 weeks, eight cycles) was compared with standard-of-care capecitabine monotherapy (1250 mg/m^2 twice a day for 14 days, every 3 weeks, eight cycles) (Figure 1).

This prospective clinical trial protocol was approved by the Korean Cancer Study Group protocol review committee (KCSG-BR18-21) and by the Ministry of Food and Drug Safety on 12 November 2018. Additional review and approval process by the institutional review boards in each institution was carried out.

Histopathological examination

The breast pathologists in each participating institution in the MIRINAE trial were asked to select and submit the most representative tumor bed section for tumor-infiltrating lymphocyte (TIL) assessment. A central review was then carried out by a dedicated breast pathologist (A. Lee), who

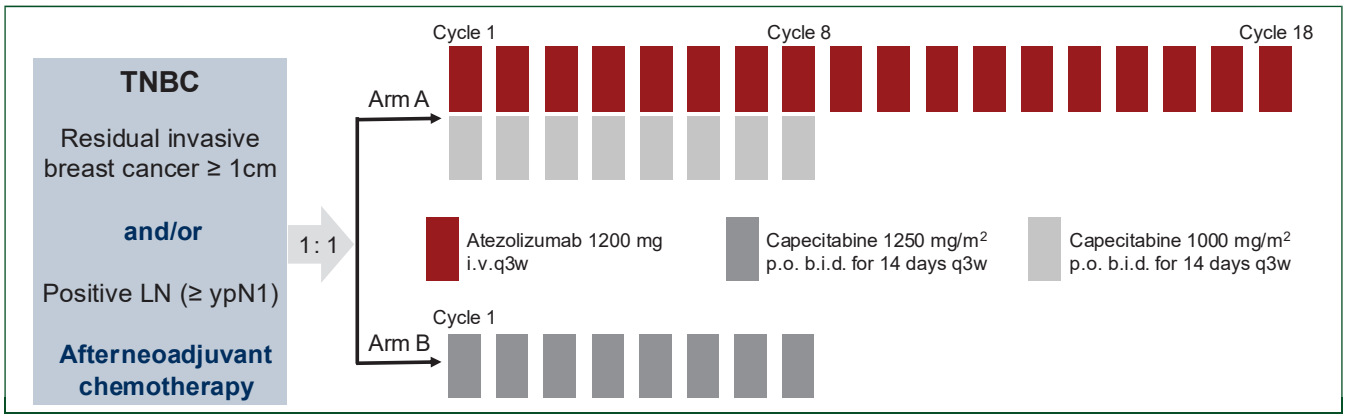

Figure 1. The scheme of the MIRINAE trial. Triple-negative breast cancer patients with residual tumors at least 1.0 cm and/or positive lymph nodes after standard neoadjuvant chemotherapy were eligible in the MIRINAE trial.
i.v., intravenous; LN, lymph node; p.o., per os; TNBC, triple-negative breast cancer.

evaluated the TILs strictly according to the International TILs Working Group 2015 guidelines.[12] A 30% cut-off was used to classify samples into TIL-high and TIL-low groups. Programmed death-ligand 1 (PD-L1) immunohistochemistry (IHC) was carried out using the clone SP142 (Ventana Medical Systems, Tucson, AZ). PD-L1 positivity was defined as PD-L1 expression in tumor cells or immune cells at a level of at least 1%.

Artificial intelligence-guided digital pathology analysis

We applied Lunit SCOPE IO (Lunit, Seoul, Republic of Korea), a deep learning-based system, to categorize the TME into three immune phenotypes (IPs). Representative hematoxylin—eosin (H&E)-stained whole-slide images (WSI) were collected for artificial intelligence-based tissue segmentation and cell detection as previously described.[13] Convolutional neural networks were used for semantic segmentation of cancer areas (CA) and cancer stroma (CS) and for cell detection, identifying tumor cells and TILs. For IP classification, each WSI was divided into 0.25 mm^2 grids, and TIL densities were assessed on the whole section, regardless of invasive margin or the tumor center. Inflamed IP was assigned if TIL density in the CA was $\geq$130/mm^2. Immune-excluded IP was defined if TIL density in CA was $<$130/mm^2 but $>$260/mm^2 in the CS. Immune-desert IP was assigned when TIL densities in both CA and CS were below their respective thresholds. WSI-level phenotypes were determined using a 33.3% cut-off for inflamed and immune-excluded scores.[14]

Targeted DNA sequencing

Formalin-fixed paraffin-embedded (FFPE) tissue samples from the surgical resection were collected for translational studies. Using the representative FFPE blocks of residual tumors, at least ten 4- to 5-µm-thick unstained sections were taken for targeted sequencing. DNA extraction, library preparation, sequencing, and bioinformatic analyses were carried out in Foundation Medicine Inc. (Cambridge, MA) using the FoundationOne CDx assay, as previously described.[15] A bioinformatician (K. Park) and a molecular pathologist (J. Koh) reviewed the sequencing reports.

RNAseq

Pathologists determined tumor purity by reviewing tumor specimens, and samples with low tumor purity (cut-off, 20%) were excluded from sequencing. Total RNA from FFPE tissues was extracted using ReliaPrep™ FFPE Total RNA Miniprep System (Promega, Madison, WI) according to the manufacturer's instructions. The quality and quantity of extracted nucleic acids were evaluated using NanoDrop™ 8000 UV—Vis spectrometer (NanoDrop Technologies Inc., Wilmington, DE), Qubit® 3.0 Fluorometer (Life Technologies, Inc., Carlsbad, CA), and 4200 TapeStation (Agilent Technologies, Santa Clara, CA).

Sequencing libraries were prepared using the Illumina TruSeq ACCESS kit (Illumina Inc., San Diego, CA) from resected FFPE specimens following the manufacturer's protocols. Paired-end sequencing of the RNA libraries was carried out on a HiSeq 2500 sequencing platform (Illumina, Inc.) at the Samsung Genome Institute (Seoul, Republic of Korea). After trimming poor-quality bases from the FASTQ files, reads were aligned to the human reference genome (hg19) with STAR v2.5.2b,[16] and estimated gene expression was calculated in terms of transcripts per million using RSEM v1.3.[17]

Molecular subtyping was conducted in terms of intrinsic subtype PAM50 via the genefu (v2.36.0) R package.[18] Additional TNBC subtyping into basal-like immune-activated (BLIA), basal-like immune suppressed (BLIS), mesenchymal (MES), and luminal androgen receptor (LAR) was carried out.[3] We also categorized TME subtypes into IE/F (immune-enriched/fibrotic), IE (immune-enriched/ non-fibrotic), F (fibrotic), and D (immune-depleted).[19] Immune cell deconvolution was carried out using CIBERSORT,[20] and comparative analyses were subsequently conducted to evaluate the proportions of individual immune cell subsets. Differentially expressed genes (DEGs) were identified using the glmFit function in the edgeR package (v4.2.1), with significance set at false-discovery rate (FDR) $<$0.01 and logCPM $\geq$2 or ≤-2. Gene set enrichment analyses (GSEA) were carried out using the ClusterProfiler (v4.12.6) and msigdbr (v7.5.1) R packages, with significance at FDR $<$0.05.

Statistical analysis

Categorical variables were analyzed by the chi-square test or Fisher's exact test, as appropriate. Continuous variables were analyzed by the Wilcoxon rank-sum or Kruskal—Wallis tests, and adjustment for multiple comparisons was carried out by the Bonferroni method. A cut-off of $P < 0.05$ was used for defining statistical significance. All statistical analyses were carried out with R version 4.4.2 (R Core Team, 2024).

RESULTS

Patient characteristics

A total of 305 patients were included in the translational analyses (Figure 2, Supplementary Table S1, available at https://doi.org/10.1016/j.esmoop.2025.105804). The median age was 48 years (range 28-74 years), and 59.0% of the patients were ≤50 years old. ypTNM (post-neoadjuvant pathological tumor—node—metastasis) stages were stage I (26.2%), II (47.9%), and III (23.3%), and HER2 IHC status was retrieved from the pathology reports from 254 patients (83.3%), where HER2-negative, 1+, and 2+ accounted for 59.1%, 29.9%, and 11.0%, respectively. PD-L1 IHC was available in 271 patients (88.9%), and 39.5% (107/271) were positive.

Genomic mutational profile and molecular subtypes

Multi-omics analyses were carried out on surgically resected residual tumors after NAC (Figure 2). We tested 277 (90.8%) samples for mutational profiling using FoundationOne®CDx, achieving a mean exon coverage of 871× (range 305×—1293×). A total of 590 oncogenic or likely oncogenic mutations were found in 108 genes. The most frequently mutated genes were *TP53* (86.3%), *PIK3CA* (18.4%), *BRCA1* (7.9%), and *PTEN* (5.8%), which was in line with the similar real-world data of Korean patients with TNBC.[21] Pathogenic alterations in the PI3K/AKT pathway (*PIK3CA*, *PTEN*, *AKT1*, and *PIK3R1*) were observed in 27.1%, and deleterious mutations in HRR-related genes (*BRCA1*, *BRCA2*, and *PALB2*) were found in 11.9%.

None of the tumors were classified as microsatellite instability-high and tumor mutational burden (TMB) ranged from 0 to 12.07 (median 3.62), with TMB-high (≥10 mutations per megabase pairs) observed in 2.2%.

RNAseq was completed for 221 patients (72.5%), achieving an average sequencing depth of 84×. RNAseq-based molecular subtyping was carried out to determine the intrinsic subtype via PAM50 and for TNBC and TME subtypes. RNAseq-based PAM50 classification revealed that 51.1% of patients were basal-like subtype, followed by luminal A (19.0%), HER2-enriched (14.0%), normal-like (10.9%), and luminal B (5.0%). According to TNBC subtyping, 36.7% of tumors were categorized as MES, followed by BLIS (30.3%), BLIA (20.8%), and LAR (12.2%). Regarding the TME, immunosuppressive subtypes D (38.1%) and F (24.4%) were predominant, followed by IE (20.8%) and a mixed IE/F type (16.7%).

We compared the genomic mutational features with RNAseq-based subtypes (Supplementary Figure S1, available at https://doi.org/10.1016/j.esmoop.2025.105804). Tumors with PI3K/AKT pathway alterations were more likely to be luminal A (34.5% versus 12.8% in non-altered, $P < 0.001$) or HER2-enriched (27.6% versus 8.1% in non-altered, $P < 0.001$) and less likely to be PAM50 basal-like subtype (25.9% versus 62.4% in non-altered, $P < 0.001$). LAR-type tumors were significantly more frequent in those with mutations in the PI3K/AKT pathway (41.4% versus 0.7% in non-altered; $P < 0.001$). Of interest, BLIS subtypes were enriched in tumors without mutations in the PI3K/AKT pathway or HRR-related genes, compared with the rest ($P < 0.001$ and $P = 0.021$, respectively).

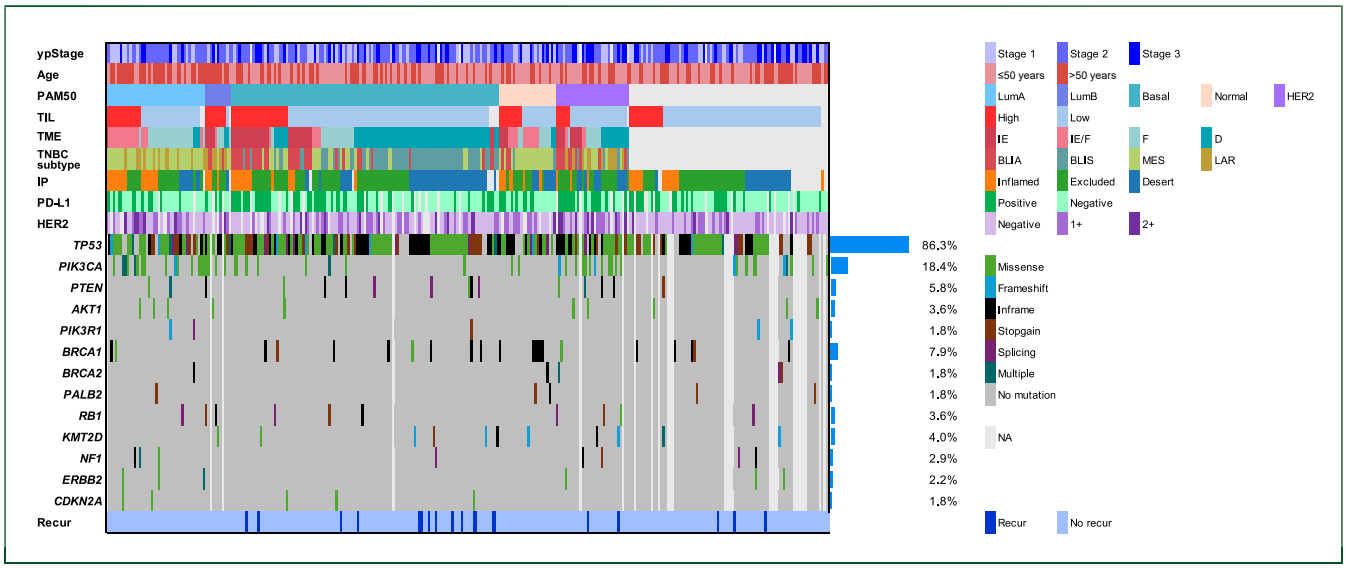

Figure 2. Genomic, transcriptomic, and histopathological features of the study population. Multi-omic profiles of 305 patients in the MIRINAE trial are shown. HER2, human epidermal growth factor receptor 2; IP, immune phenotype; NA, not assessed; PD-L1, programmed death-ligand 1; TIL, tumor-infiltrating lymphocyte; TME, tumor microenvironment.

Transcriptomic features according to tumor microenvironment

Surgical RD specimens available for H&E-based stromal TIL assessment were 299 (96.1%), with 27.1% being classified as TIL-high. PD-L1-positive tumors were infiltrated with a greater amount of TILs compared with PD-L1-negative tumors (Supplementary Figure S2, available at https://doi.org/10.1016/j.esmoop.2025.105804). Both RNAseq and TIL data were available in 213 patients (69.2%). The distribution of molecular subtypes varied relative to TIL infiltration levels (Figure 3). Although small in number, luminal B-type tumors were associated with significantly higher infiltration of TILs compared with luminal A or HER2-enriched types. The TIL-high group was significantly enriched with the BLIA subtype (37.5%; $P < 0.001$) and also in IE (45.3%) and mixed IE/F (31.3%) TME subtypes. In contrast, TIL-low tumors were predominantly associated with immune-suppressive subtypes D (49.7%) and F (29.5%) ($P < 0.001$).

To consider the spatial context of TME, we applied Lunit SCOPE IO to classify TME into three IPs: desert, excluded, and inflamed (Figure 4A). The levels of TILs were the lowest in the desert IP, and the inflamed IP had significantly more infiltration of TILs compared with the excluded IP (Figure 4B). Notably, BLIA and immune-enriched TME subtypes (IE and IE/F) were significantly enriched in the inflamed IP, suggesting spatially distinct immune profiles compared with the immune-excluded setting (Figure 4C).

Specific immune subsets were significantly enriched in the TIL-high group. CIBERSORT immune cell deconvolution analysis enabled us to see the different relative proportions of each immune subset. In TIL-high tumors, greater proportions of plasma cells, CD8+ T cells, CD4+ memory resting T cells, follicular helper T cells, activated natural killer (NK cells), and M1 macrophages were observed (all adjusted $P < 0.01$; Supplementary Figure S3, available at https://doi.org/10.1016/j.esmoop.2025.105804). Furthermore, the proportions of these six immune subsets were significantly higher in inflamed IP compared with the excluded IP (Supplementary Figure S4, available at https://doi.org/10.1016/j.esmoop.2025.105804).

We also carried out DEG analyses (Figure 4D), where TIL-high samples showed up-regulation of immune cell-related genes (*CD3D*, *CD4*, *CD8A*, *CD38*, *IRF4*, *MZB1*, and *GZMK*). Chemokine and immune checkpoint genes (*CXCL9*, *CXCL13*, and *LAG3*) were also higher in TIL-high. In contrast, *VEGFA*, *BRD4*, *CDK4*, and *IRS4* were highly expressed in TIL-low (all adjusted $P < 0.01$). According to GSEA, gene sets related to immune response and interferon-gamma response were significantly enriched in the TIL-high group. TIL-low tumors

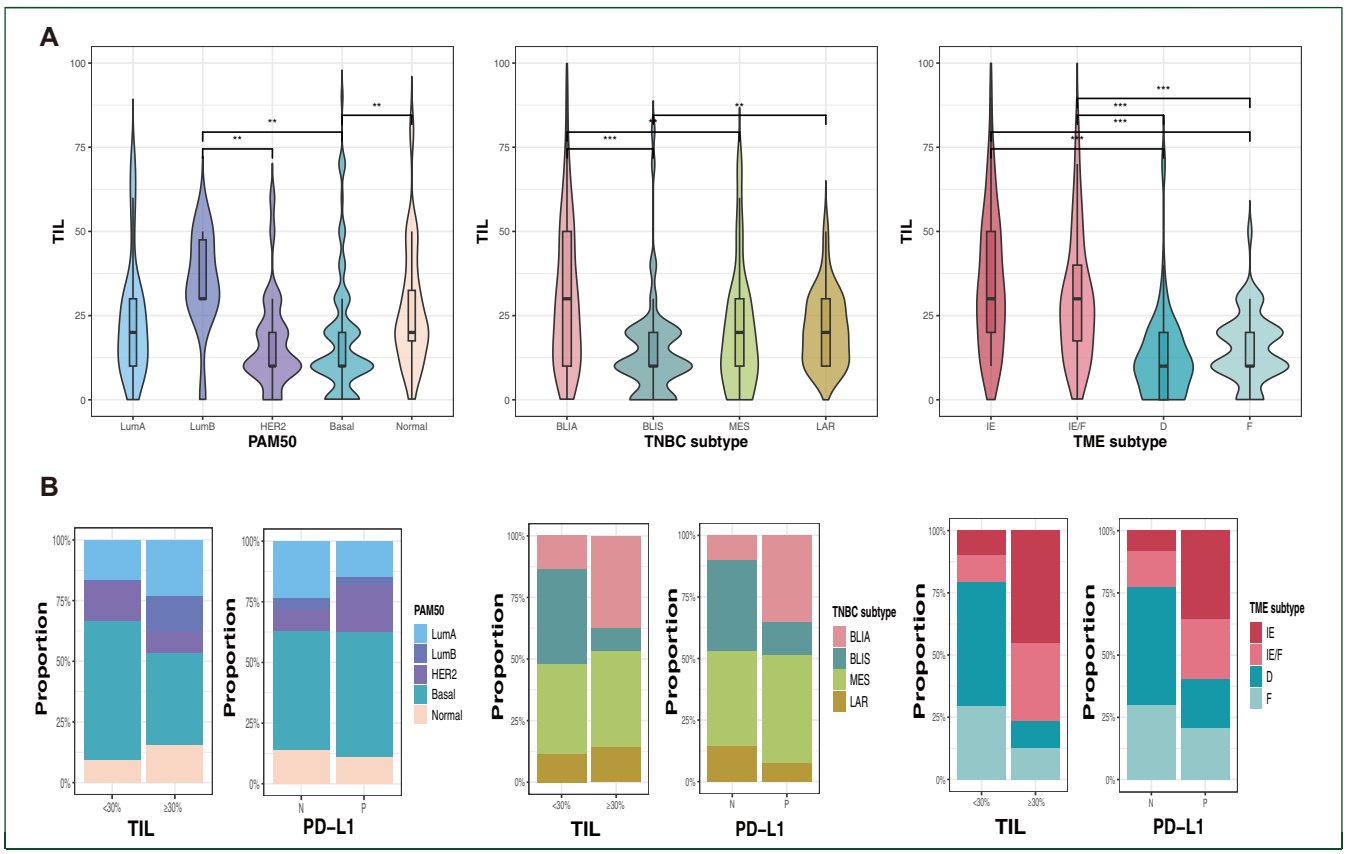

Figure 3. Tumor-infiltrating lymphocytes and PD-L1 expression according to molecular subtypes. (A, B) Luminal B by PAM50, BLIA type by TNBC classification, and IE/F or IE types by TME subtyping were associated with high TILs.
*$P < 0.05$, **$P < 0.01$, ***$P < 0.001$; ns, not significant. BLIA, basal-like immune-activated; BLIS, basal-like immune suppressed; D, immune-depleted; F, fibrotic; HER2, human epidermal growth factor receptor 2; IE, immune-enriched; IE/F, immune-enriched/fibrotic; LAR, luminal androgen receptor; MES, mesenchymal; PD-L1, programmed death-ligand 1; TIL, tumor-infiltrating lymphocyte; TME, tumor microenvironment; TNBC, triple-negative breast cancer.

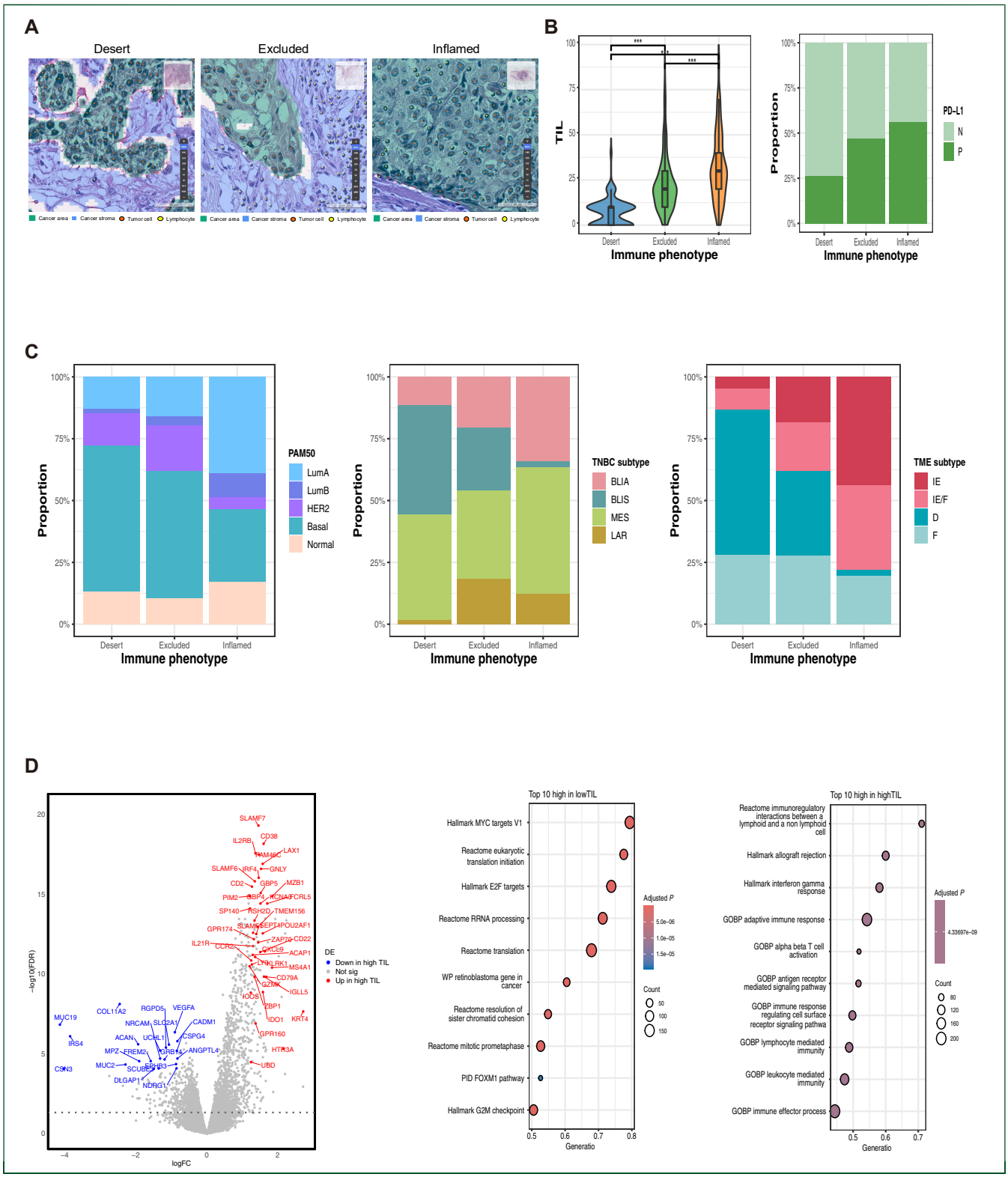

Figure 4. Characteristics of immune phenotypes of residual tumors. (A) Representative tumors in each IP are shown. (B) Stepwise increases in TILs and PD-L1 expression are found from desert, excluded, to inflamed IP. (C, D) Tumors with high TILs showed up-regulations of immune-related genes and interferon-gamma response-related gene sets.

*$P < 0.05$, **$P < 0.01$, ***$P < 0.001$; ns, not significant. BLIA, basal-like immune-activated; BLIS, basal-like immune suppressed; D, immune-depleted; F, fibrotic; HER2, human epidermal growth factor receptor 2; IE, immune-enriched; IE/F, immune-enriched/fibrotic; IP, immune phenotype; LAR, luminal androgen receptor; MES, mesenchymal; PD-L1, programmed death-ligand 1; TILs, tumor-infiltrating lymphocytes; TME, tumor microenvironment; TNBC, triple-negative breast cancer.

showed enrichment for hypoxia-related gene sets (all adjusted $P < 0.05$).

Molecular features of patients with early recurrence

To gain insights into the molecular features of residual tumors in association with the prognosis, we assessed the genomic, transcriptomic, and TME features of tumors with early recurrence, which represent primary resistance to NAC. Among the study population, 6.2% (19/305) of the patients experienced disease recurrence within 6 months after curative surgery. Characteristics of these tumors with early relapse are described in Supplementary Table S1, available at https://doi.org/10.1016/j.esmoop.2025.105804. Notably, the vast majority of these early recurrent tumors exhibited a basal-like (85.7%), BLIS (64.3%), and desert TME subtypes (71.4%) with statistical significance ($P = 0.011$, 0.007, and 0.010, respectively; Figure 5A). Furthermore, up to 71.4% of the early recurrent tumors appeared to be immune-desert IP by Lunit SCOPE IO, in contrast to 29.6% among the relapse-free group ($P = 0.002$).

Consistent with these findings, TME of the early recurrent tumors exhibited significantly lower levels of TILs ($P = 0.007$; Figure 5B). Although PD-L1 negativity was numerically higher among recurrent tumors (76.9% versus 55.9%), the difference did not reach statistical significance. Further immune cell deconvolution analysis (Figure 5C and Supplementary Figure S5, available at https://doi.org/10.1016/j.esmoop.2025.105804) revealed that early recurrent tumors were associated with lower proportions of CD4-positive naive T cells, CD4-positive memory/activated T cells ($P < 0.001$), and plasma cells ($P < 0.05$).

A total of 32 DEGs were found when comparing the early recurrent tumors to others, and early recurrent tumors showed significantly higher expression of *CCNE1*, *CD44*, *SMARCA4*, and *BRD4*. The expression of several immune function-related genes, including *CXCL12*, *IGLL5*, *CCL21*, and *CD79A* was reduced in early recurrent tumors (Figure 5D). Enrichment of gene sets representing DNA replication and MYC targets was notable in early recurrent tumors.

Taken together, our results suggest that basal-like tumors and those with less inflamed TME are more likely to relapse early during the adjuvant treatment, which warrants further in-depth clinical analyses on these tumors in each treatment arms.

DISCUSSION

In this translational study of the MIRINAE trial, we carried out histopathological examination, targeted DNA sequencing, and RNAseq followed by downstream analyses using residual TNBC samples after anthracycline and taxane-based NAC. We found that certain molecular subtypes were more prevalent in these tumors and characterized the molecular features of histopathologically immune-hot TNBC tumors.

The proportion of each subtype in TNBC varies across studies. For example, Lehmann et al. reported a distribution of 35% basal-like 1 (BL1), 22% basal-like 2 (BL2), and 25% mesenchymal (M) using TNBC type 4 subtypes.[22] In contrast, Burstein et al.[3] reported 27.3% BLIA, 30.3% BLIS, and 23.7% MES tumors. Similarly, Jiang et al.[23] reported a distribution of 24% immunomodulatory (IM), 39% BLIS, and 15% MES subtypes. Compared with these previous studies which were mostly based on primary TNBC not exposed to certain treatment, our analyses were carried out using the post-NAC residual TNBC samples. This may explain the unique features of our cohort, demonstrating a trend toward higher MES and BLIS subtypes and lower BLIA. This difference may be attributed to the clinical characteristics of our cohort, which consisted exclusively of non-pCR patients, representing a higher-risk population. For example, the immune-active BL1 subtype at baseline is reported to have the highest pCR rate compared with other subtypes,[24] which may explain why our cohort showed reduced prevalence of BLIA. Additionally, the distribution of subtypes in our cohort may reflect molecular subtype changes during NAC, for it is well known that significant dynamic changes occur following cytotoxic chemotherapy.[25,26] This trend in molecular subtypes is even more pronounced in early recurrent tumors, where the BLIS subtype is particularly elevated. Consequently, our cohort is enriched with tumors exhibiting a high-risk TME.

To see which types of immune subsets are more predominant in TME of TIL-high tumors, we carried out CIBERSORT immune cell virtual deconvolution and found higher proportions of plasma cells, CD8+ T cells, CD4+ memory resting T cells, follicular helper T cells, activated NK cells, and M1 macrophages. Interestingly, these six immune subsets were significantly more abundant in the immune-inflamed IP compared with the immune-excluded IP, suggesting the role of these immune subsets in the proximity of tumor cells.

The residual tumors of the patients who relapsed within 6 months of disease-free survival had lower levels of TIL infiltration and were enriched with immune-desert IP by the Lunit SCOPE IO classification. Furthermore, these tumors were enriched with basal-like, BLIS, and desert TME subtypes. Although additional clinical data and length of survival should be taken into investigation, our current data suggest that tumors having histopathologically immune-cold features harbor a greater risk of early recurrence, and that gene expression-based molecular subtyping can also aid in prognostication of these patients.

A limitation of this study is that patients in the MIRINAE trial did not receive pembrolizumab as part of NAC, which has now become a standard of care per KEYNOTE-522.[7] Thus, our findings may not fully reflect TME changes induced by neoadjuvant immunotherapy. However, given global variability in NAC regimens, characterizing residual TNBC in non-ICI-treated patients remains clinically relevant. Identifying shared

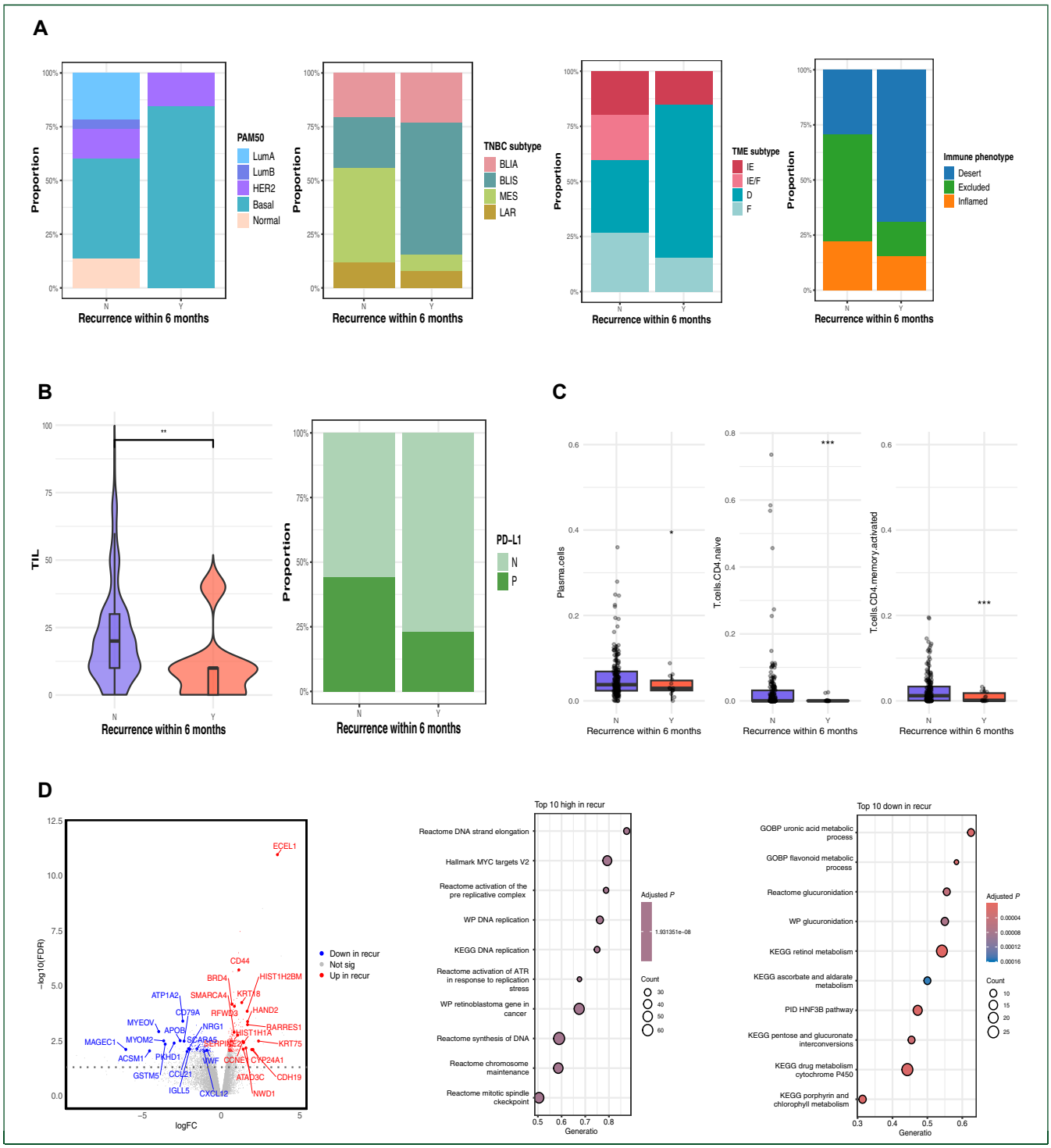

Figure 5. Characteristics of tumors with early recurrence within 6 months after curative surgery. (A) Early recurrent tumors were significantly enriched with basal-like, BLIS type, D subtype, and desert IP. (B) Low levels of TILs are found in early recurrent tumors. (C, D) Genes and gene sets toward cellular proliferation characterize tumors with early recurrence.
BLIA, basal-like immune-activated; BLIS, basal-like immune suppressed; D, immune-depleted; F, fibrotic; HER2, human epidermal growth factor receptor 2; IE, immune-enriched; IE/F, immune-enriched/fibrotic; IP, immune phenotype; LAR, luminal androgen receptor; MES, mesenchymal; PD-L1, programmed death-ligand 1; TILs, tumor-infiltrating lymphocytes; TME, tumor microenvironment; TNBC, triple-negative breast cancer.

molecular features between NAC-ICI and non-ICI-treated TNBC may provide insights for optimizing adjuvant strategies. Future studies should compare residual TNBC across NAC regimens to refine risk stratification and identify predictive biomarkers for recurrence and therapy response.

Conclusion

In this study, we presented genomic, transcriptomic, and histopathological characteristics of residual TNBC tumors treated with standard NAC in the prospective, multicenter, phase II MIRINAE trial. Residual invasive tumors were

predominantly basal-like or MES/BLIS subtypes with TME features toward less immune response. Early recurrence was associated with immune-cold TME, which suggests the crucial need for advanced therapeutic strategies in these tumors. Ongoing analyses of each treatment arm along with the complete clinicopathological data will provide deeper insights into the role of ICI as an adjuvant treatment.

FUNDING

This work was supported by the National R&D Program for Cancer Control through the National Cancer Center (NCC), funded by the Ministry of Health & Welfare, Republic of Korea [grant number RS-2022-CC127321].

DISCLOSURE

SAI received research fund from AstraZeneca, Boryung, Daiichi Sankyo, Eisai, Roche, and Pfizer outside of this research work; has advisory role for AstraZeneca, Daiichi Sankyo, Eisai, Eli Lilly, GSK, MSD, Novartis, Roche, and Pfizer outside of this research work. JK has advisory role for AstraZeneca outside of this research work. KHJ declares an advisory role and consultant for AstraZeneca, Bixink, Daiichi Sankyo, Gilead, Novartis, F. Hoffmann-La Roche, MSD, Pfizer, Eisai, and Takeda. JL declares research grants from Pfizer and Celltrion; consulting fees from Gilead, Amgen, Roche, Lilly, Pfizer, Novartis, and Daiichi Sankyo; payment or honoraria for lectures, presentations, or educational events from Eisai, Boryung, Lilly, AstraZeneca, Pfizer, Novartis, MSD, Celltrion, and Daiichi Sankyo. HKA declares consulting fees from Gilead, Amgen, Roche, Takeda, Daewoong, Bayer, Lilly, and Daiichi Sankyo; and payment or honoraria for lectures, presentations, speakers bureaus, or educational events from Eisai, Boryung, Lilly, LSK Korea, AstraZeneca, Yuhan, Pfizer, Novartis, Sanofi/Aventis, MSD, Boehringer Ingelheim, Celltrion, and Daiichi Sankyo. JHK declares research grants (funding) from Ono Pharmaceuticals Ltd, Eisai Korea, and Roche and received consulting or advisory role for Bixink, Eisai, Everest Medicine, MSD, Roche, Yuhan, and AstraZeneca; honoraria from Roche Korea, AstraZeneca, Roche diagnostics, Lilly Korea, and Amgengrants or contracts from Roche, Ono Pharmaceuticals, and Eisai paid to their institution; consulting fees from AstraZeneca, Eisai, MSD, Everest Medicine, and Roche; and payment or honoraria for lectures, presentations, speakers bureaus, or educational events from Roche Korea, AstraZeneca, Roche diagnostics, Lilly Korea, and Amgen. KHP declares advisory role for AstraZeneca, Amgen, Eli Lilly and Company, F. Hoffmann-La Roche AG, Daiichi Sankyo, Novartis, and Pfizer. KSL declares consulting fees from Novartis, Daiichi Sankyo, Gilead Sciences, AstraZeneca, Pfizer, and Everest Medicines. JS declares grants or contracts from Seagen, MSD, Roche, Pfizer, Novartis, AstraZeneca, Lilly, GSK, Boehringer Ingelheim, Sanofi, Daiichi Sankyo, Qurient, Dragonfly, Eikon, Gilead, Celcuity, BMS, HLB Life Science, Sermonix Pharmaceuticals, Olema, Hanmi Pharm, Ildong Pharmaceutical, and Samyang Holding paid to their institution; and that an immediate family member has stock or stock options in Daiichi Sankyo. KJS declares advisory role for AstraZeneca, Eisai, and Eli Lilly and Company. SBK declares grants or contracts from Novartis, Sanofi Aventis, and DongKook Pharm; consulting fees from Novartis, AstraZeneca, Lilly, Dae Hwa Pharmaceutical, ISU Abxis, OBI Pharma, Beigene, and Daiichi Sankyo; payment or honoraria for lectures, presentations, speakers bureaus, or educational events from Novartis, AstraZeneca, Lilly, OBI Pharma, and Daiichi Sankyo; and stock or stock options in Genopeaks and Neogene TC. KHL declares consulting fees from MSD and payment or honoraria for lectures, presentations, speakers bureaus, or educational events from AstraZeneca, Eisai, Lilly, Novartis, Pfizer, and Roche. YHP declares grants or contracts from MSD, Novartis, Pfizer, AstraZeneca, Roch, Gencurix, and Inocras; consulting fees from AstraZeneca, MSD, Pfizer, Eisai, Lilly, Roche, Gilead, Daiichi Sankyo, MENARINI, Everest Medicine, and Novartis; payment or honoraria for lectures, presentations, speakers bureaus, manuscript writing, or educational events from AstraZeneca, MSD, Pfizer, Roche, Lilly, Daiichi Sankyo, Novartis, Gilead, and Helsinn; support for attending meetings or travel from Gilead, AstraZeneca, and Pfizer; participation on a data and safety monitoring board or advisory board for AstraZeneca, MENARINI, Pfizer, Novartis, Roche, Daiichi Sankyo, and Helsinn; and receipt of equipment, materials, drugs, medical writing, gifts, or other services from Dong-A ST, Sanofi, Roche, and Pfizer. IHP received research funding from Roche. All other authors have declared no conflicts of interest.

DATA SHARING

All the data generated or analyzed during this study are available from the corresponding authors on reasonable request.

REFERENCES

1. Sung H, Ferlay J, Siegel RL, et al. Global cancer statistics 2020: GLOBOCAN estimates of incidence and mortality worldwide for 36 cancers in 185 countries. *CA Cancer J Clin*. 2021;71:209-249.
2. Lehmann BD, Bauer JA, Chen X, et al. Identification of human triple-negative breast cancer subtypes and preclinical models for selection of targeted therapies. *J Clin Invest*. 2011;121:2750-2767.
3. Burstein MD, Tsimelzon A, Poage GM, et al. Comprehensive genomic analysis identifies novel subtypes and targets of triple-negative breast cancer. *Clin Cancer Res*. 2015;21:1688-1698.
4. Pantelidou C, Sonzogni O, Taveira MDO, et al. PARP inhibitor efficacy depends on CD8+ T-cell recruitment via intratumoral STING pathway activation in BRCA-deficient models of triple-negative breast cancer. *Cancer Discov*. 2019;9:722-737.
5. Houssami N, Macaskill P, Minckwitz G von, Marinovich ML, Mamounas E. Meta-analysis of the association of breast cancer subtype and pathologic complete response to neoadjuvant chemotherapy. *Eur J Cancer*. 2012;48:3342-3354.
6. Minckwitz G von, Schneeweiss A, Loibl S, et al. Neoadjuvant carboplatin in patients with triple-negative and HER2-positive early breast cancer (GeparSixto; GBG 66): a randomised phase 2 trial. *Lancet Oncol*. 2014;15:747-756.
7. Schmid P, Cortes J, Pusztai L, et al. Pembrolizumab for early triple-negative breast cancer. *N Engl J Med*. 2020;382:810-821.

8. Schmid P, Cortes J, Dent R, et al. Event-free survival with pembrolizumab in early triple-negative breast cancer. *N Engl J Med*. 2022;386:556-567.
9. Schmid P, Cortes J, Dent R, et al. Overall survival with pembrolizumab in early-stage triple-negative breast cancer. *N Engl J Med*. 2024;391:1981-1991.
10. Norikazu M, Soo-Jung L, Shoichiro O, et al. Adjuvant capecitabine for breast cancer after preoperative chemotherapy. *N Engl J Med*. 2017;376:2147-2159.
11. Ignatiadis M, Bailey A, McArthur H, et al. Adjuvant atezolizumab for early triple-negative breast cancer. *JAMA*. 2025;333.
12. Salgado R, Denkert C, Demaria S, et al. The evaluation of tumor-infiltrating lymphocytes (TILs) in breast cancer: recommendations by an International TILs Working Group 2014. *Ann Oncol*. 2015;26:259-271.
13. Bang YH, Lee CK, Bang K, et al. Artificial intelligence-powered spatial analysis of tumor-infiltrating lymphocytes as a potential biomarker for immune checkpoint inhibitors in patients with biliary tract cancer. *Clin Cancer Res*. 2024;30:4635-4643.
14. Shen J, Choi YL, Lee T, et al. Inflamed immune phenotype predicts favorable clinical outcomes of immune checkpoint inhibitor therapy across multiple cancer types. *J Immunother Cancer*. 2024;12:e008339.
15. Milbury CA, Creeden J, Yip WK, et al. Clinical and analytical validation of FoundationOne®CDx, a comprehensive genomic profiling assay for solid tumors. *PLoS One*. 2022;17:e0264138.
16. Dobin A, Davis CA, Schlesinger F, et al. STAR: ultrafast universal RNA-seq aligner. *Bioinformatics*. 2013;29:15-21.
17. Li B, Dewey CN. RSEM: accurate transcript quantification from RNA-Seq data with or without a reference. *BMC Bioinformatics*. 2011;12:323.
18. Gendoo DMA, Ratanasirigulchai N, Schröder MS, et al. Genefu: an R/Bioconductor package for computation of gene expression-based signatures in breast cancer. *Bioinformatics*. 2015;32:1097-1099.
19. Bagaev A, Kotlov N, Nomie K, et al. Conserved pan-cancer microenvironment subtypes predict response to immunotherapy. *Cancer Cell*. 2021;39:845-865.e7.
20. Newman AM, Steen CB, Liu CL, et al. Determining cell type abundance and expression from bulk tissues with digital cytometry. *Nat Biotechnol*. 2019;37:773-782.
21. Koh J, Kim J, Woo GU, et al. Harnessing institutionally developed clinical targeted sequencing to improve patient survival in breast cancer: a seven-year experience. *Cancer Res Treat*. 2024;57:443-456.
22. Lehmann BD, Jovanović B, Chen X, et al. Refinement of triple-negative breast cancer molecular subtypes: implications for neoadjuvant chemotherapy selection. *PLoS One*. 2016;11:e0157368.
23. Jiang YZ, Ma D, Suo C, et al. Genomic and transcriptomic landscape of triple-negative breast cancers: subtypes and treatment strategies. *Cancer Cell*. 2019;35:428-440.e5.
24. Masuda H, Baggerly KA, Wang Y, et al. Differential response to neoadjuvant chemotherapy among 7 triple-negative breast cancer molecular subtypes. *Clin Cancer Res*. 2013;19:5533-5540.
25. Park YH, Lal S, Lee JE, et al. Chemotherapy induces dynamic immune responses in breast cancers that impact treatment outcome. *Nat Commun*. 2020;11:6175.
26. Masuda H, Harano K, Miura S, et al. Changes in triple-negative breast cancer molecular subtypes in patients without pathologic complete response after neoadjuvant systemic chemotherapy. *JCO Precis Oncol*. 2022;6:e2000368.